

## SUCCESSIVE EJECTION EVENTS IN THE L1551 MOLECULAR OUTFLOW

R. BACHILLER,<sup>1</sup> M. TAFALLA,<sup>1,2</sup> AND J. CERNICHAO<sup>1</sup>

Received 1993 November 12; accepted 1994 February 4

### ABSTRACT

We report CO  $J = 2 \rightarrow 1$  strip maps along the axis and across the lobes of the L1551 molecular outflow. The overall structure of the outflow is more complicated than previously believed. In particular, we find at least four successive high-velocity features along the axis of the blueshifted lobe which are very suggestive of different ejection episodes. The well-known “shell structure” is restricted to the feature closest to the exciting source, indicating that a simple hollow shell model is inappropriate to explain the overall outflow structure. In contrast, our data are more consistent with recent jet-driven models for bipolar outflows. The presence of different high-velocity features suggest that the entraining jet could be of intermittent nature.

We have also carried out high-sensitivity observations of  $^{13}\text{CO}$  toward selected positions in the outflow, and we infer from them that self-absorption effects in the CO wing profiles are unimportant.

*Subject headings:* ISM: individual (L1551) — ISM: jets and outflows — stars: formation — stars: pre-main-sequence

### 1. INTRODUCTION

The bipolar outflow in the Taurus cloud L1551 (distance 160 pc; Snell 1981) is the best studied bipolar outflow around any young stellar object. The observations of this remarkable outflow have provided for a long time the basis for most of the theoretical work carried out to model the structure, origin, and evolution of bipolar outflows (Cabrit & Bertout 1986; Uchida et al. 1987; Shu et al. 1991). In fact, the high-velocity CO emission in L1551 shows a systematic pattern: the highest velocity emission is mainly located toward the middle of both lobes, while the lower velocity gas appears along the edges leaving a large central “hole” (see, e.g., Figs. 4–6 of Moriarty-Schieven et al. 1987). Indeed, at first sight, the most straightforward interpretation of such a peculiar velocity pattern is that each lobe of the outflow is an empty inflating bubble with the CO emission arising at the expanding shell. This has been a widely accepted interpretation (Snell, 1987; Moriarty-Schieven et al. 1987; Uchida et al. 1987; Fridlund et al. 1989, etc.) and has made the hollow shell picture remain for a long time as the conventional framework for the interpretation of bipolar outflows. The hollow shell models, however, present major drawbacks (see discussion in Bachiller & Gómez-González 1992), and an alternative picture of outflows driven by highly collimated jets is now emerging (Stahler 1993; Masson & Chernin 1993; Raga & Cabrit 1993).

To further probe the structure of the L1551 outflow, we have observed in CO, with high angular resolution, strips along the outflow axis and across the lobes. We find that the blueshifted lobe is more complicated than previously believed. It presents evidence for multiple eruption events, and its structure seems more consistent with recent jet-driven models than with the old hollow shell picture.

In addition, we have carried out high-sensitivity observations of some selected positions in  $^{13}\text{CO}$ , since it had been previously suggested that the  $^{12}\text{CO}$  wing emission could be

affected by self-absorption (Fridlund & White 1989). We find this is probably not the case.

### 2. OBSERVATIONS

The observations were carried out with the IRAM 30 m telescope at Pico Veleta (near Granada, Spain) in 1993 May. We used an SiS receiver tuned at the CO  $J = 2 \rightarrow 1$  frequency near 230 GHz, with a noise temperature about 150 K (SSB). Typical SSB system temperatures above the atmosphere, and corrected for attenuation losses, were 600–800 K. The antenna HPBW and the beam efficiency were 12" and 0.45 at such frequency. The spectrometer was an autocorrelator giving a spectral resolution of 39 kHz ( $0.051 \text{ km s}^{-1}$  at 230 GHz). Some selected positions were simultaneously observed in  $^{13}\text{CO}$   $J = 2 \rightarrow 1$  by using another similar SiS receiver tuned near 220 GHz, followed by another autocorrelator identical to the one used to observe the CO 230 GHz line. The spectra were obtained by position switching. We observed several strip maps with a spacing of 28". Pointing was frequently checked on nearby continuum sources and was found to be accurate within 3". Calibration was achieved by the chopper wheel method. Only linear baselines have been removed from the spectra. All intensities are reported in units of main beam brightness temperature. After the preanalysis phase, we smoothed the spectra to a velocity resolution of about  $0.3 \text{ km s}^{-1}$ .

### 3. OVERALL OUTFLOW STRUCTURE

The  $^{12}\text{CO}$   $J = 2 \rightarrow 1$  strip map along the main outflow axis is shown in Figure 1. Both the red- and blueshifted outflow lobes exhibit bright emission, and there is little overlap between them, confirming that the inclination of the outflow to the line of sight is large. The appearance of each lobe, however, is very different. The striking morphology of the blueshifted lobe is discussed in § 4. The redshifted lobe, on the other hand, presents a relatively simple structure: the terminal velocity of the wings increases with distance to the source up to 6' and then decreases in a quite symmetrical way. In addition, the wings present a small dip at velocities between 10 and 14  $\text{km s}^{-1}$ . This configuration reminds of an expanding bubble or shell, but we stress, however, that (i) such a “bubble” is not an

<sup>1</sup> Centro Astronómico de Yebes (IGN), Apartado 148. E-19080 Guadajara, Spain.

<sup>2</sup> Postal address: Astronomy Department, University of California at Berkeley, 601 Campbell Hall, Berkeley, CA 94720.

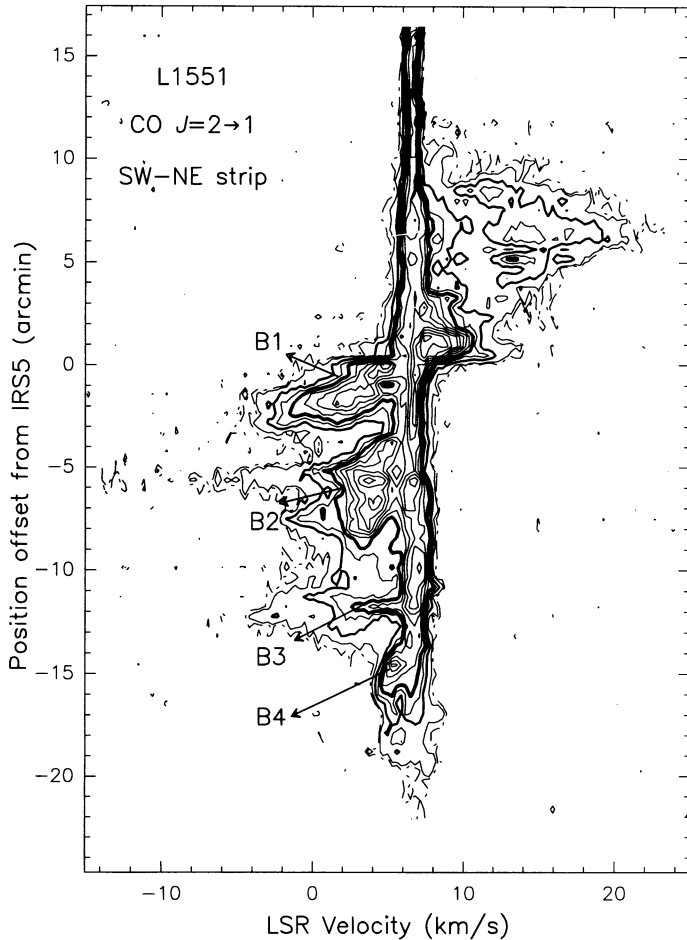


FIG. 1.—Velocity-position diagram along a SW-NE line, i.e., close to the main L1551 outflow axis, in the CO  $2 \rightarrow 1$  line. Position offsets are in arcseconds with respect to IRS 5, which is  $04^{\circ}28^{\text{m}}40^{\text{s}}.1$ ,  $18^{\circ}01'41''.2$  (1950.0). Contours are at 1 K (dash), 1.5, 3 (thick), 4.5, 6 (thick), ... etc. B1, B2, B3, and B4 are the high-velocity features discussed in the text.

empty structure, since there is strong CO emission at intermediate velocities, and (ii) it has a very irregular geometry, as it presents obvious signs of clumpiness. A similar distribution is also seen in the strip map across the redshifted outflow presented in Figure 2a.

An interesting issue is the obvious lack of symmetry between the two lobes of high velocity gas (Fig. 1). The redshifted lobe stops suddenly at about  $12'$  from the central source, whereas the blueshifted lobe extends beyond  $18'$ , all the way to the edge of the cloud. The blueshifted gas, in fact, seems to be escaping from the cloud, since the lines are weak and broad at the positions near the lobe termination, and there is not a clear “ambient” cloud component in that region (a similar conclusion was reached by Moriarty-Schieven & Snell 1988, from a different data set). In contrast, the ambient component remains very strong and narrow beyond the redshifted lobe termination (upper region of the diagram in Fig. 1), as if the quiescent ambient gas were contraining the expansion of the red outflow. It is thus very likely that the asymmetry observed in the outflow results from an asymmetry in the gas distribution of the ambient cloud.

Another interesting effect is that the ambient cloud line is narrower toward positions beyond the edge of redshifted lobe

than toward positions on the lobe. This clearly indicates that the bipolar outflow contributes significantly to the line width of the ambient component inside the outflow region (see also Myers et al. 1988, and Tafalla, Bachiller, & Martín-Pintado 1993).

One could worry about the possible influence of opacity effects in the CO profile shapes. In fact, Fridlund & White (1989) have suggested that self-absorption effects could be distorting the CO profiles, which could lead to a misinterpretation of the structure and kinematics of the outflow. Such a difficulty could be surmounted by observing the optically thin lines of  $^{13}\text{CO}$ , but the wing emission in such lines is very weak. Figure 3 shows  $^{13}\text{CO}$  spectra compared to the corresponding  $^{12}\text{CO}$  profiles for some selected positions in the outflow. The  $^{12}\text{CO}/^{13}\text{CO}$  intensity ratio increases from a value of about 2 at ambient velocities, to values of 10–15 in the inner regions of the wings, and to even higher values ( $\geq 20$ –40) in the outer wings; such ratios indicate that the  $^{12}\text{CO}$  emission is optically thin at the highest velocities, but that it can be moderately thick in the inner wings ( $^{12}\text{CO } J = 2 \rightarrow 1$  opacities in the range 1–10, depending upon the gas kinetic temperature). The  $^{12}\text{CO}$  and  $^{13}\text{CO}$  profile shapes, on the other hand, are similar in all the positions observed, except toward  $(-200'', -40'')$ . We note, however, that this position lies at the edge of the brightest clump in the strip map of Figure 2b, and that slight changes in the pointing or in the size and shape of the telescope beam (due in particular to the different frequencies of the  $^{12}\text{CO}$  and  $^{13}\text{CO}$  lines) may suffice to produce significant differences between the profiles of the two isotopes at this particularly critical edge position. We therefore conclude that the  $^{12}\text{CO}$  and  $^{13}\text{CO}$  profile shapes are predominantly similar, and that  $^{12}\text{CO}$  self-reversals, if any, are unimportant in the wing emission. This conclusion contradicts that reached by Fridlund & White from less sensitive  $^{13}\text{CO}$  observations.

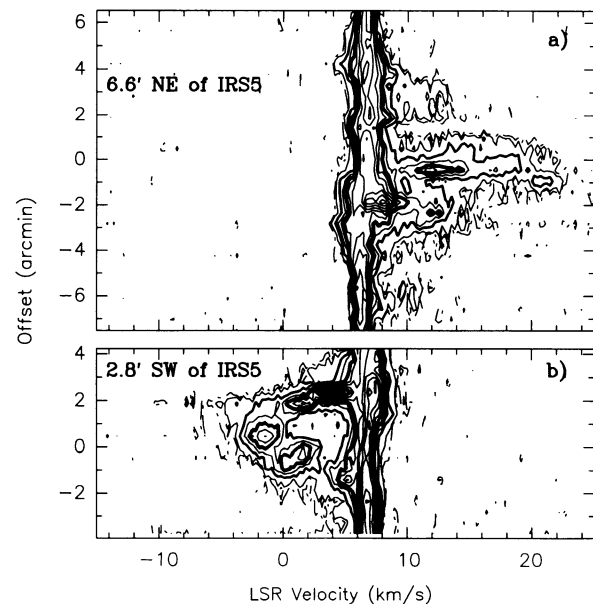


FIG. 2.—Velocity-position diagrams along cuts perpendicular to the outflow axis centered at (a)  $6.6'$  northeast of IRS 5 (i.e., passing through the redshifted lobe) and (b)  $2.8'$  southwest of IRS 5 (i.e., cutting the blueshifted lobe at the edge of B1). Position offsets are in arcseconds with respect to the position on the outflow axis. Contours and map spacing are as in Fig. 1.

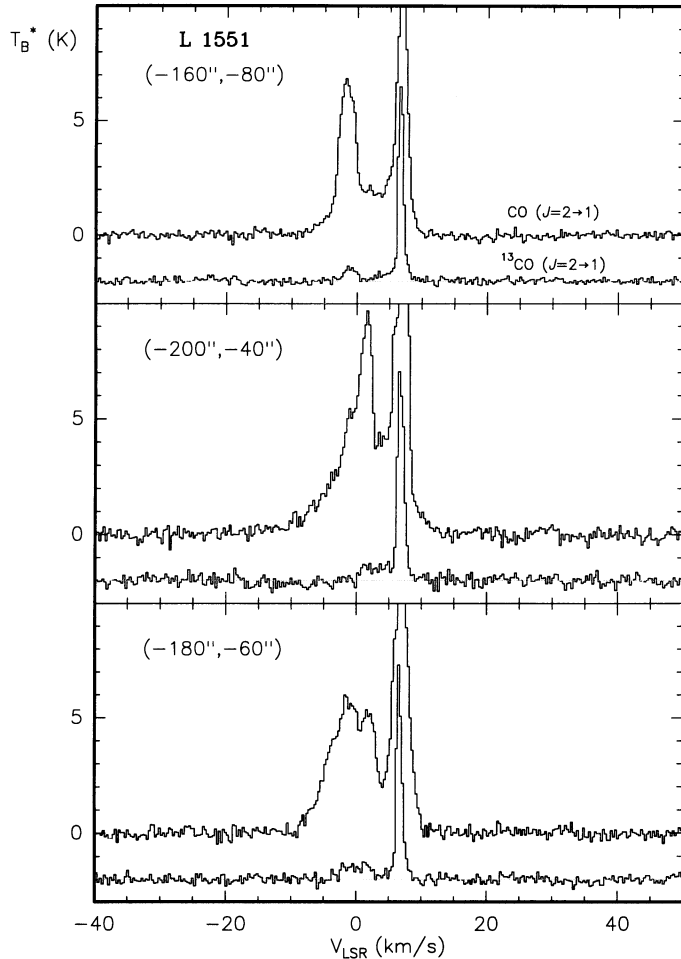


FIG. 3.—CO and  $^{13}\text{CO}$   $J = 2 \rightarrow 1$  spectra obtained toward selected positions in the L1551 outflow. Offsets are in arcseconds from IRS 5.

#### 4. SUCCESSIVE EJECTION EVENTS

The map of the blueshifted gas in Figure 1 reveals a highly complex structure. At least four well-defined high-velocity (HV) features are observed along the lobe axis and have been labeled B1, B2, B3, and B4 in the map. This structure clearly indicates that the high-velocity gas is not homogeneously distributed in the lobe. Rather, the distinct maxima do correspond to different lumps of outflowing material. Velocity-position diagrams produced across the lobe at different distances from the star are shown in Figure 2. Particularly interesting is the strip map at  $2.8'$  southwest of the star (Fig. 2b). This diagram reveals a remarkable ring-shaped structure very suggestive of a shell. This is the shell structure which has been widely studied previously (e.g., Moriarty-Shieven et al. 1987; Uchida et al. 1987), and which is coincident with an optical and infrared nebula formed by the reflexion of the stellar light in the cavity walls (e.g., Campbell et al. 1988). The present observations reveal the shell is very clumpy (about five clumps are well observed in the “ring” of Fig. 2b), in good agreement with the  $3 \rightarrow 2$  observations of Parker et al. (1991). We notice, however, that the shell picture is valid only for feature B1, i.e., for a small portion of the blueshifted lobe, and that the new features B2, B3, and B4 do not fit within a scenario of a unique shell. Feature B2 is spatially very extended ( $\sim 6'$ ), and is well seen in a CO  $J = 1 \rightarrow 0$  strip map made by Uchida et al. (1987). However,

features B3 and B4 are not clearly seen in their observations; though these can be perceived in the maps by Moriarty-Shieven & Snell (1988, see their Fig. 5). The present observations were carried out with higher angular and spectral resolutions, making easier the detection of the weaker features B3 and B4, and provide much more details on the four HV features.

From the present observations, it is possible to obtain an estimate of the kinematical age of each HV feature as  $R \tan i / V_R$ , where  $R$  is the distance of the lump centroid to the exciting star,  $i$ , is the inclination of the outflow axis to the plane of the sky ( $16^\circ$  according to Liseau & Sandell 1986), and  $V_R$  is the mean radial velocity of the HV feature. For a distance of 160 pc, we find that the age of B4, the oldest feature, is about  $10^5$  yr, and that the time elapsed between successive ejections is  $2\text{--}3 \times 10^4$  yr. These timescales for the molecular outflow are considerably larger than those observed for the optical jet, which is much faster (velocities of  $300\text{--}700 \text{ km s}^{-1}$  have been measured for L1551; Campbell et al. 1988), but carries a considerably smaller amount of mass (resulting in a momentum which could be comparable to that of the molecular outflow).

It is noticeable that the terminal velocity of the successive HV features decreases with distance to IRS 5, which suggests that the gas could be decelerating as it moves away from the source. (If such deceleration is real, the age estimates of the previous paragraph should be shortened in accordance.) On the other hand, the velocity field *within* every HV feature seems to present a systematic acceleration, since the terminal flow velocity, as well as the mean velocity, both increase with distance to the source in B1, B2, and B4 (the kinematics of B3 remains essentially unresolved by the present observations). This acceleration effect has also been observed in other bipolar outflows. Different authors (Shu et al. 1991; Masson & Chernin 1992) have referred to this acceleration as a “Hubble law,” because it is approximately linear with distance, and have interpreted it as generated by density gradients in the ambient clouds. However, Stahler (1994) explains this acceleration effect in the frame of jet-driven molecular outflows and claims that such acceleration is a natural result of the turbulent entrainment process. It is interesting to note that the different HV features in the L1551 blue lobe exhibit different “Hubble laws.”

The individual mass of each HV feature is a parameter of considerable interest, but it is not well constrained by our observations, since complete maps are necessary to make accurate estimates. From mapping observations, Fridlund et al. (1989) estimated a mass of  $0.6\text{--}1.1 M_\odot$  for B1 and most of the B2 feature. B3 and B4 are probably less massive and would contain a few tenths of  $M_\odot$ . Despite all the uncertainties, the mass of the blueshifted lobe most likely exceeds  $1 M_\odot$ .

To summarize, the presence of four successive HV features in the L1551 blue lobe strongly suggests that the L1551 outflow has passed through four main activity epochs. The duration of each mass-loss epoch, and the time elapsed between two of them, is about a few  $10^4$  yr. The molecular material associated with each HV feature presents a high degree of clumpiness, and its mass likely ranges from a few tenths to  $1 M_\odot$ .

The HV features in the L1551 outflow provide a clear piece of evidence that episodic mass-loss phenomena play an important role in bipolar outflows. The observational evidence for intermittent events in molecular outflows and in optical jets, in fact, starts to be well documented: high-velocity CO clumps have been observed along the axes of several bipolar molecular outflows (Bachiller et al. 1990; Bachiller, Martin-Pintado, &

Planesas 1991; Richer, Hills, & Padman 1992; André et al. 1990); discrete high-velocity components have been found by means of near-IR spectroscopy of young objects (Mitchell, Maillard, & Hasegawa 1991); and successive shocked knots, believed to be due to recurrent eruptive events, have been observed in some optical jets (e.g., Reipurth, Raga, & Heathcote 1992; Bally, Lada, & Lane 1993), including the L1551 jet (Campbell et al. 1988; Neckel & Staude 1987). The timescales of these transient phenomena, however, are much shorter than those of the activity epochs reported here. Our observations suggest that the intermittency of the outflow phenomenon is not limited to small transient events, but it extends over periods of activity and quiescence comparable to the total outflow age. The L1551 outflow appears to vary at all timescales.

#### 5. HOLLOW SHELLS VERSUS JET-DRIVEN OUTFLOWS

Our observations also underscore the complexity of the L1551 outflow. Certainly some portions of the outflow lobes resemble expanding shells, but we stress that such “shell” structures should be *filled* with molecular gas (since relatively strong CO emission is observed at intermediate velocities; see Figs. 1 and 2). In addition, a hollow shell model presents other major problems as, for example, it cannot explain naturally the absence of a velocity component corresponding to the back sides of the shells. It is clear then, that an empty cavity model is inappropriate to explain the overall structure of the L1551 outflow. On the other hand, (i) the fact that the maximum

values of the radial velocity are observed towards the main outflow axis (see transverse strip maps in Fig. 2), and (ii) the high value of the collimation degree (the ratio of the outflow to its width), which is likely in the range 5–8, as revealed by the present high-resolution observations, make the structure of the L1551 outflow much better explainable with a model in which a central driving jet is entraining the ambient material. First theoretical descriptions of such models have been made available recently (Stahler 1993; Masson & Chernin 1993; Raga & Cabrit 1993). The jet-driving models provide a good explanation for the observed velocity field in L1551 (with the highest velocities at the outflow axis) and do not need an ad hoc geometry, as the shell model does. Moreover, such models also explain the increase of the radial velocity away from the driving star (Stahler 1994).

In summary, it appears that the hollow shell picture for L1551 has been clouding for a long time the true relation between the molecular outflow and the variable optical jet known to be at its axis. The presence of successive HV features along the blueshifted lobe is a dominant aspect of the L1551 flow and considerably impact our previous ideas on the structure of this prototypical outflow. Our observations strongly suggest that the entraining jet in the L1551 outflow could be of intermittent nature.

We are grateful to the IRAM staff at Pico Veleta for help during the observations. This research has been partially supported by the Spanish CICYT (project PB 90-0408).

#### REFERENCES

- André, P., Martín-Pintado, J., Despois, D., & Montmerle, T. 1990, *A&A*, 236, 180  
 Bachiller, R., Cernicharo, J., Martín-Pintado, J., Tafalla, M., & Lazareff, B. 1990, *A&A*, 231, 174  
 Bachiller, R., & Gómez-González, J. 1992, *Astron. & Astrophys. Rev.*, 3, 257  
 Bachiller, R., Martín-Pintado, J., & Planesas, P. 1991, *A&A*, 251, 639  
 Bally, J., Lada, E. A., & Lane, A. P. 1993, *ApJ*, 418, 322  
 Cabrit, S., & Bertout, C. 1986, *ApJ*, 307, 313  
 Campbell, B., Persson, S. E., Strom, S. E., & Grasdalen, G. L. 1988, *AJ*, 95, 1173  
 Fridlund, C. V. M., Sandqvist, A., Nordh, H. L., & Olofsson, G. 1989, *A&A*, 213, 310  
 Fridlund, C. V. M., & White, G. J. 1989, *A&A*, 223, L13  
 Liseau, R., & Sandell, G. 1986, *ApJ*, 304, 459  
 Masson, C. R., & Chernin, L. M. 1992, *ApJ*, 387, L47  
 ———. 1993, *ApJ*, 414, 230  
 Mitchell, G. F., Maillard, J. P., & Hasegawa, T. I. 1991, *ApJ*, 371, 342  
 Moriarty-Schieven, G. H., & Snell, R. L. 1988, *ApJ*, 332, 364  
 Moriarty-Schieven, G. H., Snell, R. L., Strom, S. E., Schloerb, F. P., Strom, K. M., & Grasdalen, G. L. 1987, *ApJ*, 319, 742  
 Myers, P. C., Heyer, M., Snell, R. L., & Goldsmith, P. F. 1988, *ApJ*, 324, 907  
 Neckel, J., & Staude, H. J. 1987, *ApJ*, 322, L27  
 Parker, N. D., White, G. J., Hayashi, S. S., & Williams, P. G. 1991, *A&A*, 250, 134  
 Raga, A., & Cabrit, S. 1993, *A&A*, 278, 267  
 Reipurth, B., Raga, A. C., & Heathcote, S. 1992, *ApJ*, 392, 145  
 Richer, J. S., Hills, R. E., & Padman, R. 1992, *MNRAS*, 254, 525  
 Shu, F. H., Ruden, S. P., Lada, C. J., & Lizano, S. 1991, *ApJ*, 370, L31  
 Snell, R. L. 1981, *ApJS*, 45, 121  
 ———. 1987, in *IAU Symp. 115, Star-Forming Regions*, ed. M. Peimbert & J. Jugaku (Dordrecht: Reidel), 213  
 Stahler, S. W. 1993, in *Astrophysical Jets*, ed. M. Livio, O’Dea & D. Bugarella (Cambridge: Cambridge Univ. Press), in press  
 ———. 1994, *ApJ*, 422, 616  
 Tafalla, M., Bachiller, R., & Martín-Pintado, J. 1993, *ApJ*, 403, 175  
 Uchida, Y., Kaifu, N., Shibata, K., Hayashi, S. S., Hasegawa, T., & Hamatake, H. 1987, *PASJ*, 39, 907